Tumor Associated Mesenchymal Stromal Cells Show Higher Immunosuppressive and Angiogenic Properties Compared to Adipose Derived MSCs

Ladan Langroudi[1], Zuhair Muhammad Hassan[1]*, Masoud Soleimani[2], Seyed Mahmoud Hashemi[3]

[1]Department of Immunology, [2]Department of Hematology, Faculty of Medical Sciences, Tarbiat Modares University, [3]Department of Immunology, School of Medicine, Shahid Beheshti University of Medical Sciences, Tehran, Iran

ABSTRACT

Background: Differentiation, migratory properties and availability of Mesenchymal Stromal Cells (MSC) have become an important part of biomedical research. However, the functional heterogeneity of cells derived from different tissues has hampered providing definitive phenotypic markers for these cells. **Objective:** To characterize and compare the phenotype and cytokines of adipose derived MSCs (AD-MSCs) and tumoral-MSCs (T-MSCs) isolated from mammary tumors of BALB/c mice. **Methods:** Immunophenotyping and in vitro differentiation tests were used for MSC characterization. Cytokine and enzyme profiles were assessed using ELISA and Real-time PCR, respectively. **Results**: T-MSCs expressed significantly higher levels of HLA-DR ($p=0.04$). Higher levels of PGE2 and COX-2 enzyme were also observed in T-MSCs ($p=0.07$ and $p=0.00$, respectively). Additionally, T-MSCs expressed higher levels of iNOS and MMP9 ($p=0.01$ and $p=0.01$, respectively). T-MSCs were also able to induce higher levels of proliferation and migration of HUVEC endothelial cells in wound scratch assay compared to AD-MSCs ($p=0.015$). **Conclusion**: Functional differences showed by the surface markers of MSCs, cytokine and enzyme production indicate the effect of different microenvironments on MSCs phenotype and function.

Langroudi L,et al. Iran J Immunol. 2015; 12(4):226-239.

Keywords: Adipose-Derived Mesenchymal Stromal Cells, Breast Cancer, Immunomodulatory Properties, Tumoral-MSCs

---

*Corresponding author: Dr.Zuhir Muhammad Hassan, Department of Immunology, Faculty of Medical Sciences, Tarbiat Modares University, Tehran, Iran. Tel: (+) 98 21 82883565, Fax: (+) 98 21 82884550, email: hasan_zm@modares.ac.ir

INTRODUCTION

Mesenchymal stromal cells (MSCs) are self-renewable, multi-potent fibroblastic cells (1), which under defined conditions, are able to differentiate into various lineages *in vitro* including osteogenic (2), chondrogenic (3), adipogenic (4), myogenic (5) and recently neurogenic (6) and epithelial (7) cells. Being readily available from different tissues such as adipose and bone marrow, various studies have taken the advantage of *in vitro* differentiation for regenerative repair of injured tissues (8). *In vivo*, however, they have diverse roles in tissue repair and inflammation. When required, local or bone marrow MSCs migrate to the site of inflammation or injury and depending on the microenvironment can produce an array of growth factors inducing angiogenesis, regeneration, remodeling, immune cell activation or suppression, and cellular recruitment (9-11). They lack the expression of MHC molecules (12), are resistant to NK (Natural Killer cell) and CTL (cytotxic T cell) lysis and suppress CD8 maturation (13). Studies have shown that they do not induce activation molecules on T cells and suppress the production of IFN-γ (14). MSCs suppress immune reactions via cell-independent mechanisms and through soluble mediators (15), induce differentiation of iTregs (16) and a Th2 pattern of immune response (17). In addition, soluble mediators and suppressive enzymes such as TGF-β, IDO and COX-2 play roles in the immune-suppression of MSCs (18). Thus, they have attracted much attention and hope for cell therapy. The fact that they migrate to the site of inflammation or injury and modulate the milieu, prompted many studies to utilize MSCs in gene or drug delivery systems (10). Numerous animal and human studies have exploited the possibility of therapeutic gene delivery in various disease settings. Many of these evaluations have shown encouraging results. However, there are results that contradict the efficacy of MSCs *in vivo* (19). This discrepancy calls for further research into the biology of MSCs and the roles they play in various microenvironments.

Microenvironment or niche is the term describing the landscape of *in vivo*, which is very much different in cellular composition, signals and interactions from *in vitro* conditions. Since microenvironment can affect the gene expression of engrafted cells, it could variably impact cell therapies using MSCs.

In the cancerous niche, many factors are involved in the growth of transformed cells. Recently, inflammation was added as one of the hallmarks of cancer (20). It has many roles in initiation and development of cancer. Diverse cell populations beside cancer cells are involved in the tumor microenvironment. Fibroblasts, Mesenchymal cells, pericytes and cells of the immune system contribute to the inflammatory milieu of cancer (21). The landscape of cancer is very eluded and unresponsive. Under the influence of many factors mentioned above and many unknown factors, informative studies on various factors of cancer are beneficial for future therapeutic developments. As MSCs gain more interest in the field of cancer therapy, knowing and understanding the niche before transferring an armed cell is advisable. Therefore, this study aimed to compare the immune properties of murine adipose derived-MSCs (AD-MSCs) and the tumoral MSCs (T-MSCs). AD-MSCs and T-MSCs show similar morphology and differentiation, however, T-MSCs have higher expression of COX-2 enzyme and T-MSCs show higher angiogenic properties compared to AD-MSCs. The tumor model used was SMMT (spontaneous mouse mammary tumour), which is a non-chemical, spontaneous mammary tumor of BALB/c mouse reserved by routine subcutaneous syngenic transplantations.

MATERIALS AND METHODS

Tumour Model and Mesenchymal Cell Isolation. 4-6 weeks old female BALB/c mice (Pasture Institute, Tehran, Iran) were subcutaneously transplanted with SMMT tissue (22). After 4 weeks, when the tumors reached a size of 400 mm^3, mice were sacrificed. Tumor tissue was washed in PBS and minced with scalpel into 1-3 mm sized fragments. Then, 20-25 pieces of tumor fragments were cultured per T75 flasks coated with 0.1% gelatin. After attachment of tissues, 5ml Dulbecco minimum essential medium/F12 (DMEM/F12) (GIBCO, USA) supplemented with 30% fetal bovine serum (FBS) (GIBCO, USA) and 1% penicillin/streptomycin (Biosera, UK) was added. For two consecutive days, additional 5 ml media was added to each flask. Fibroblastic cells grew out of the explants and after a week the tissues were removed and fibroblastic colonies were passaged in 10% FBS DMEM/F12. These cells were characterized and used for future evaluations.AD-MSCs were harvested from peritoneal adipose of BALB/c healthy adult female mice (6–8 weeks). The adipose tissue was aseptically removed. Adipose tissue explants were used for isolation of AD-MSCs in DMEM+30% FBS and gelatin-coated flasks as described above.

MSC Characterization. Several methods were used to characterize MSCs as follows:

1. Immunostaining and FACS Analysis. To analyze the cell surface expression of MSC markers, the following antibodies were used: PE conjugated anti-CD29, anti-CD105, anti-HLA-DR, anti-CD44; FITC conjugated anti-CD104a, anti-CD45, anti-Sca-1and anti-CD11b (eBioscience). Cells were divided into aliquots (5×10^5each), stained with FITC- or PE-conjugated antibodies at final concentration of 1µg/ml at room temperature for 30 min, washed with PBS. Results were analyzed by BD FACS flow cytometry and Flowjo software.

2. Differentiation of MSCs *in Vitro*. To evaluate osteogenic differentiation, 70-80% confluent MSCs were incubated in osteogenic media (DMEM supplemented with 10% FBS, 10 mM b-glycerol phosphate, 1 nM dexamethasone and 0.5µMascorbate 2-phosphate) for four weeks with media changed twice a week. The cells were fixed with 3.7% paraformaldehyde (PFA) and stained with Alizarin Red (pH= 4.1).

To induce adipogenic differentiation, 70-80% confluent MSCs were incubated in adipogenic media (DMEM supplemented with 10% FBS, 0.5 mM isobutylmethylxanthine (IBMX), 66 nM insulin, 10^{-7}M dexamethasone and 0.2nM indomethacin) for four weeks and the media was changed twice a week. The cells were fixed in 3.7% PFA and stained with 0.5% Oil Red.

Chondrogenic differentiation was evaluated by culturing 10^6 cells in chondrogenic media (DMEM supplemented with TGF-β 10 ng/ml, ascorbic acid 50 µg/ml and 10^{-7}M dexamethasone) for four weeks and the media was changed twice a week. The cell pellet was fixed in 10% formalin, sectioned and stained with Alcian blue.

3. Colony Forming Unit-Fibroblast (CFU-F) Assay. The CFU-F assay was performed using a modification of a described protocol(23). MSCs were cultured in three concentrations of 100, 500 and 1000 viable cells in 10cm dish for two weeks. The medium was changed twice per week. On the 14th day, cultures were fixed with 4% PFA and stained with crystal violet. Fibroblastic colonies with more than 50 cells and or possessing a diameter greater than 2mm were counted under an inverted microscope. Three separate T-MSCs and AD-MSC samples were evaluated in triplicate.

4. Growth Curve. MSCs were cultured in DMEM at an initial density of 5000 per well in 24 well plates. At 24-hour intervals, standard MTT assay was performed and the optical density was measured at 570 nm with a reference wavelength reading at 630 nm. The OD measurements were corrected using a standard cell curve. The growth curve was evaluated for 12 consecutive days.

5. Cytokine Production. The conditioned medium of MSCs 70-80% confluent culture at passage 2, was collected and analyzed for the levels of IL-10, IL-17, TGF-β, and Prostaglandin E2 using ELISA kit (DuoSet ELISA Development kit, R&D systems, Minneapolis, MN, USA). All procedures were followed according to the manufacturer's protocol.

6. Nitric Oxide Production. We measured NO levels (nmol/ml) in culture supernatants by the Griess reaction. Briefly, nitrite was measured by adding equal volumes of Griess reagent (1% sulphanilamide and 0.1% naphthylenediamine in 5% phosphoric acid) to conditioned media samples. The optical density at 550 nm was measured by usinga microplate reader. The concentrations were calculated by comparison with the standard solutions of sodium nitrite prepared in the culture medium. Fresh mediumwas used as blank to subtract background absorbance of NO produced by MCSs. All chemicals were obtained from Merck (Darmstadt, Germany).

Gene Expression Assay by Real-Time PCR. After both MSCs were isolated, total cellular RNA was isolated using Trizol (Gibco-BRL, Life Technologies, MD). Random hexamer-primed reverse transcription (Metabion) was performed on aliquots (1 μg) of total RNA as a template. The resulting cDNA was used for PCR amplification. Primers for cycloxygenase 2 (COX-2), inducible nitric oxide synthetase (iNOS), indolamine deoxygenase (IDO), matrix metalloproteinase 2 (MMP2) and 9 (MMP9) and beta-actin were synthesized based on the reported sequences (should provide reference for each primer set).

COX-2 (145 bp)
forward: AGACAGATCATAAGCGAGGAC,
reverse: CCACCAATGACCTGATATTTC;

INOS (142):
forward: TGTGCGAAGTGTCAGTGG,
reverse: TCCTTTGAGCCCTTTGTG;

IDO (168 bp):
forward: GGATGCGTGACTTTGTGG,
reverse: TGGAAGATGCTGCTCTGG;

MMP2 (150 bp):
forward: AGACAAGTTCTGGAGATACAATG,
reverse: GCACCCTTGAAGAAGTAGC;

MMP9 (136 bp):
forward: GGCGTGTCTGGAGATTCG,
reverse: TGGCAGAAATAGGCTTTGTC.

Real-time PCR reaction mixtures (final volume of 30 ul) contained 1 µl cDNA, 30 pmol of each primer, 3 µl of 200 µM dNTP, and 1U Taq-DNA polymerase (MBI FermentasInc., Burlington, ON). Amplification conditions were as follows: 25 cycles of 94°C for 30 s; 55°C for 60 s; and 72°C for 1 min, followed by 72°C incubation for 10 min.

***In vitro* Wound Healing Assay.** To test the ability of MSCs to induce endothelial proliferation and migration, HUVEC cell line was used for scratch test assay. HUVECs were cultured in 6 well plates. When confluent monolayer was completed, using a sterile tip, the monolayer was disrupted, leaving an acellular line in the middle of the well. HUVECs were treated with the conditioned medium of AD-MSCs, T-MSCs, 4T1 and VEGF (10ng/ml). The scratch line was photographed at 0, 4, 24, 48 and 72 hours. The percent of wound closure relative to hour 0 was measured using image J software.

Statistical Analysis. Results were calculated as a mean of at least three independent experiments and are expressed as mean±SEM. A $p<0.05$ was considered statistically significant using ANOVA test in SPSS statics 19 software (SPSS Inc., Chicago, IL).

RESULTS

T-MSC and AD-MSCs Showed Similar Morphology and Characteristics. MSCs were isolated and cultured as described. The explants showed fibroblastic-like outgrowths after 7 days of culture. Isolated MSCs presented a spindle shape and a homogenous population in culture (Figure 1). Passage 3 cells were used in characterization protocols using flowcytometry analysis and adipocytic, osteocytic and chondrogenic differentiation tests.

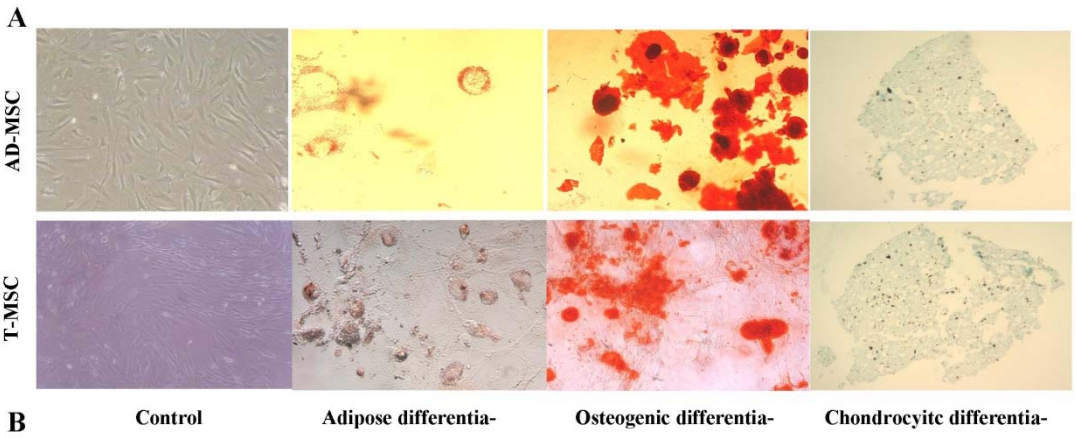

Figure 1. Phase contrast microscopy of AD-MSCs (A) and T-MSCs (B) at passage 2. **Adipogenic differentiation was determined by Oil Red O staining for lipid vacuoles. Differentiation into osteocytes after induction culture was assessed by Alizarin Red S staining for calcium mineralization. Chondrocytic differentiation was evaluated by Alcian Blue staining of cell pellets treated with induction media. Control cultures in normal growth medium were also stained and were negative (data not shown). The figure shows one representative results from 3 independent experiments.**

Figure 2. Surface markers of isolated MSCs. 10^5 cells were stained with FITC- or PE-labeled antibodies to mouse CD29, CD105, CD90, HLA-DR,

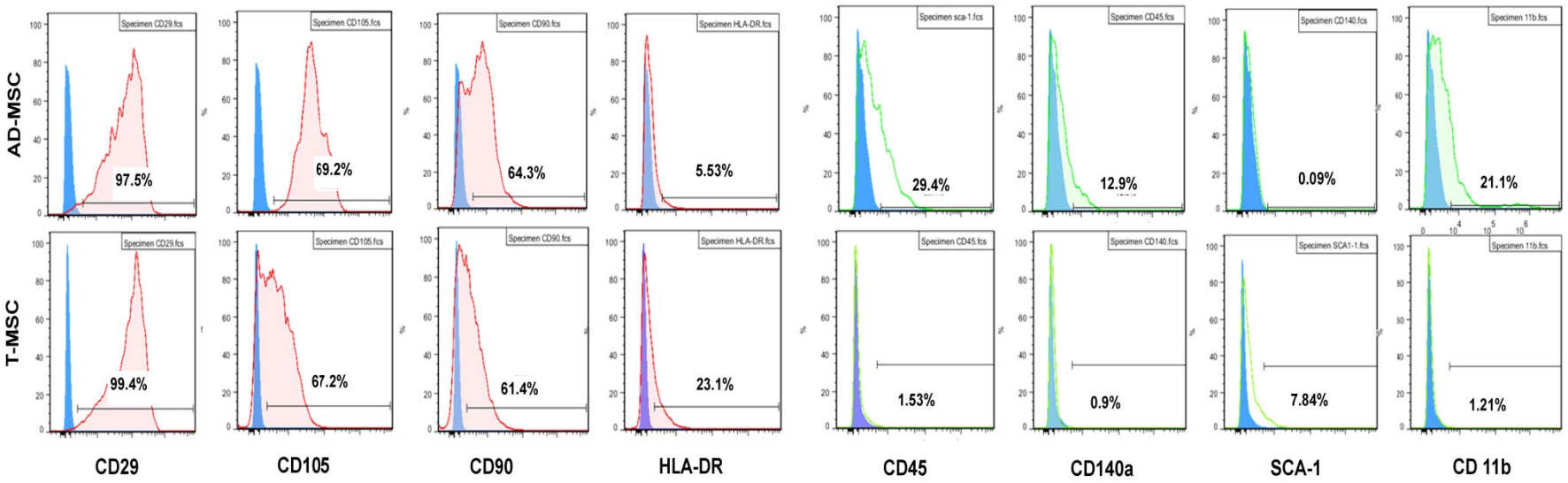

CD45, CD140a, Sca-1 and CD11b. Flowcytometry analysis was performed in triplicate using ABI system and Flowjo software. Results revealed similar phenotypes with slightly elevated levels of HLA-DR in T-MSCs.

1.Suface Marker Expression. Flowcytometry analysis for stromal cell specific markers revealed that both AD-MSCs and T-MSCs express CD29, CD105, CD90 and partially Sca-1. They were negative for CD11b and CD45 (Figure 2). However, T-MSCs expressed slightly elevated levels of HLA-DR (23.1 ± 8% in T-MSCs vs. 5.5±3 % in AD-MSCs).

2.*In Vitro* Cell Differentiation. MSCs were exposed to osteoblast-, adipocyte- and chondrocyte-induction medium. MSCs formed aggregates and calcium deposits after 3 weeks and Alizarin red staining for calcium salt was positive for osteogenic differentiation.

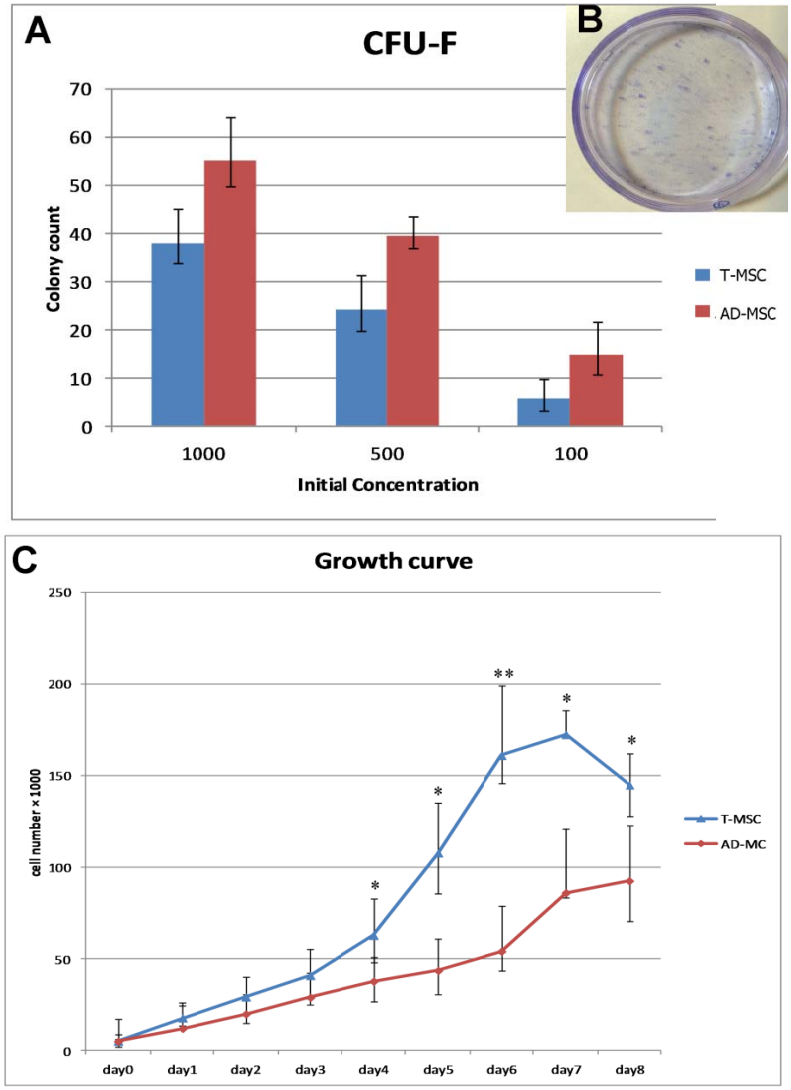

Figure3. the ability to proliferate *in vitro* was evaluated using colony forming unit-fibroblastic (CFU-F) (A and B) and growth curve (C) assays. Both AD-MSCs and T-MSCs showed similar abilities in colony forming and proliferation. Statistical analysis showed no significant difference between the numbers of colonies each MSC was able to form (p values were 0.3, 0.4 and 0.9 for cell concentrations of 1000, 500 and 100 cells/dish respectively).

However in growth curve assay, T-MSCs showed higher amount of MTT reduction which could point to a higher metabolic rate in T-MSCs compared to AD-MSCs ($p<0.05$).

The ability to differentiate into adipocytes was similar among derived MSCs. Chondrocytic differentiation was evaluated using Alcian blue staining of section slides. Both MSCs showed the ability to produce chondrogenic ECM (Figure 1).

3. Colony Forming Ability. The ability of AD-MSCs and T-MSCs to form fibroblastic colonies was evaluated using a CFU-F assay. The number of CFU-F cells obtained at passage 3 is shown in Figure 3A and B. CFU-F assay was performed in three cell inoculum concentrations; 1000, 500,100 cells/dish.

Number of colonies was counted in three separate experiments for each MSC. Statistical analysis showed no significant difference between the numbers of colonies each MSC was able to form. (p values for 1000 cell: 0.35, for 500 cells: 0.4 and for 100 cells were 0.9). However, the number of colonies were lower in tumor derived MSCs.

4. Growth Curve. For 12 consecutive days, proliferations of 5000 seeded cells were evaluated using MTT assay. The optical density was corrected using a MTT-cell standard curve. Statistical analysis showed that the growth of T-MSCs was significantly higher compared to AD-MSCs (Figure 3C). The difference was significant after 4 days of culture ($p=0.002$). Curve equation evaluations calculated the doubling time of AD-MSC as 2.5 and T-MSCs as 1.7 days.

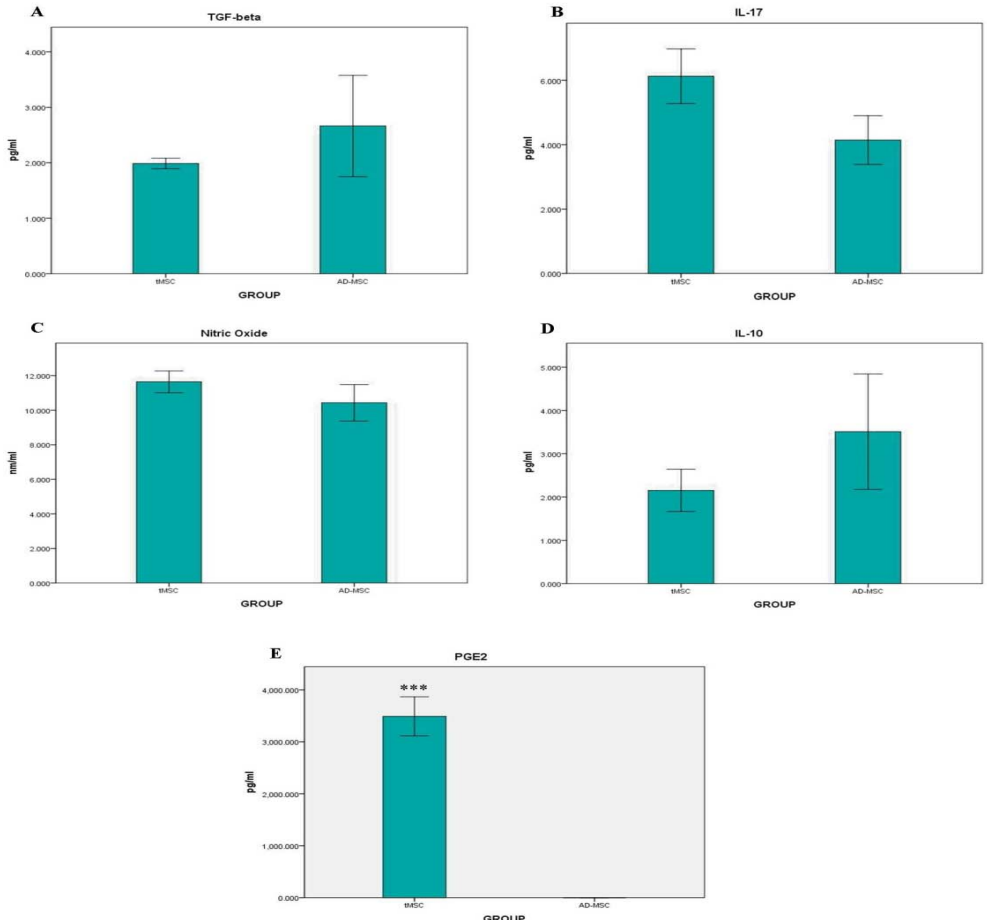

Figure4. cytokine pattern of T-MSCs and AD-MSCs *in vitro* was evaluated using ELISA. Both MSCs had similar pattern of TGF-β (A), IL-17 (B), Nitric Oxide (C) and IL-10 (D) production

(p=0.9) except for PGE2 (E) which significantly higher levels of production was seen in T-MSCs (p=0.007).

Different Functional Properties between T-MSC and AD-MSCs.

1. Cytokine Production. The levels of cytokines produced by each MSC were evaluated by ELISA (Figure 4).

Statistical analysis revealed no difference between the production of IL-10, IL-17, TGF-β and nitric oxide (p=0.9). However, the production of PGE2 was higher in the T-MSCs culture (p= 0.007).

2. Gene Expression Analysis. The relative mRNA expressions and the heatmap comparison of the enzymes iNOS, IDO, COX-2, MMP9 and MMP2 are shown in Figure 5. The relative expressions were analyzed in REST software and R studio was used to demonstrate the heatmap of gene expression comparison. The results revealed that the median expression of MMP9, COX-2 and iNOS was significantly higher in T-MSCs (MMP9: 6.105 folds, COX-2: 164.849 folds and INOS: 10.447 folds higher with a p value of 0.000 for COX-2 and 0.01 for MMP9 and iNOS).

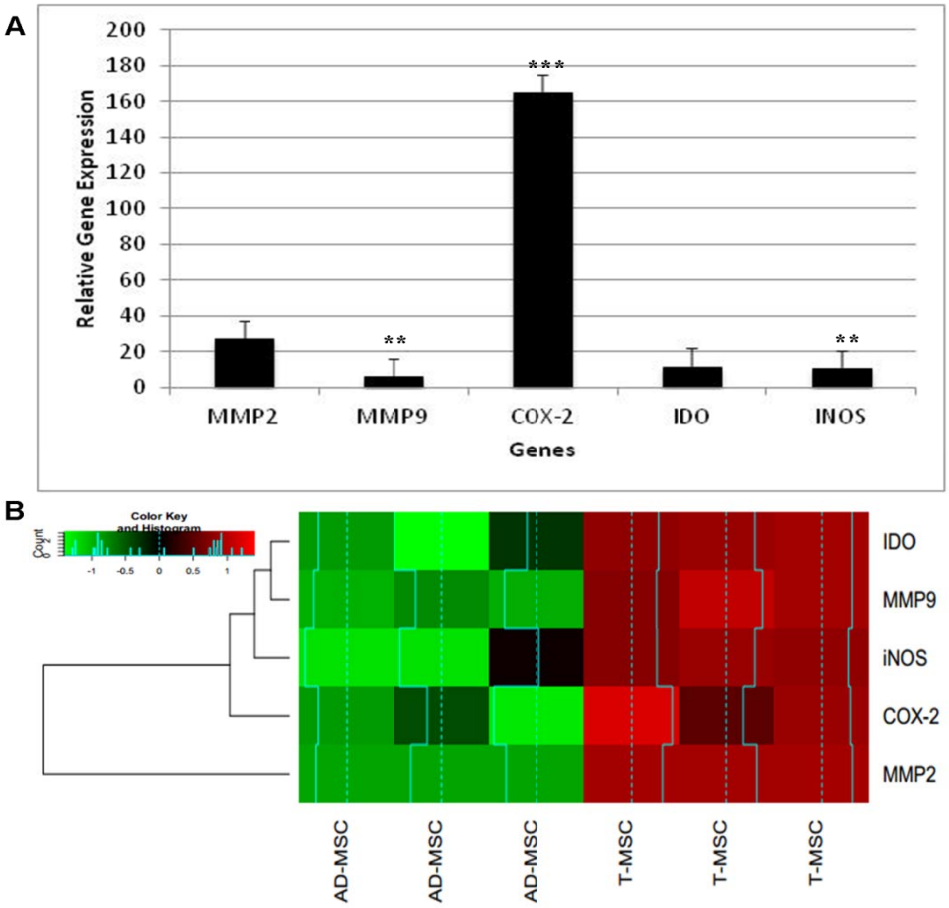

Figure5. relative gene expression (A) and Heatmap (B) comparison of MMP2, MMP9, COX-2, IDO and iNOS expression. mRNAs were extracted from T-MSCs and AD-MSCs in passage 2. cDNA was synthesized and Real-Time PCR was used to compare gene expressions. AD-MSCs were used as the control as a normal cell and T-MSCs as the target.

Significant increase was observed in the expression of COX-2, MMP9 and iNOS with 164.849, 6.105 and 10.447 folds higher expression in T-MSCs compared to AD-MSCs (***: p= 0.000, **: p=0.01).

3.*In Vitro* Wound Healing Properties. Treatment with conditioned medium of T-MSC and AD-MSC was used to evaluate the ability of cellular products to support angiogenesis *in vitro*. The most effective treatment was VEGF, with 73% and 100% closure in 24 and 48 hours, respectively (p=0.02 compared to T-MSC and 4T1). Similar results were observed with T-MSC and 4T1 treatment (75.5% and 57.69% in 24 hours and 81.78% and 75.34/5 in 48 hours and 88.02% and 78.23% wound closure in 72 hours respectively). However, treatment with AD-MSC conditioned medium was less effective in inducing HUVEC migration and proliferation (21.80%in 24 hours, 37.62% in 48 hours and 36.80% in 72 hours). The difference between AD-MSC and T-MSC-induced wound closure was statistically significant (p=0.015).

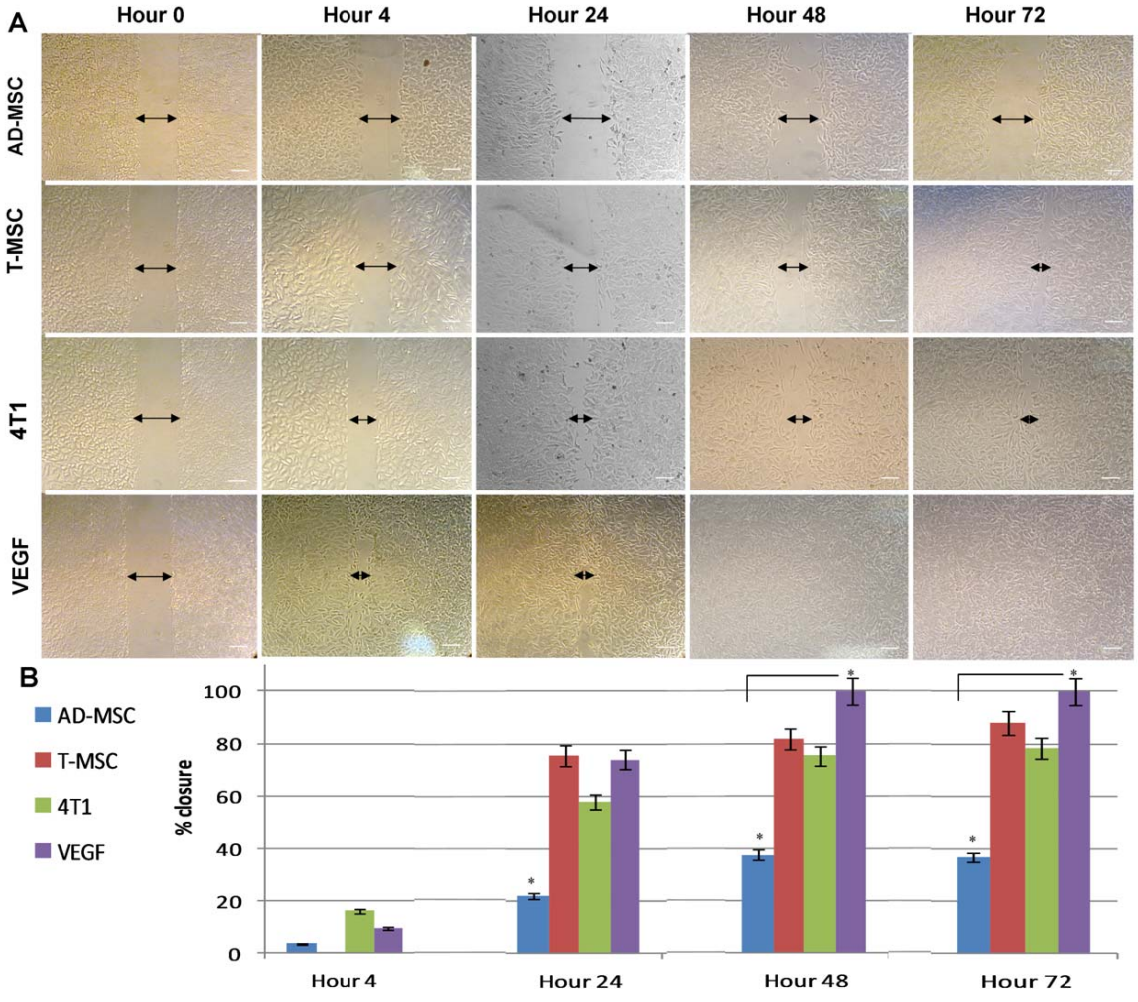

Figure 6. *In vitro* wound healing assay was assessed using HUVEC culture. Confluent HUVEC culture was treated with conditioned media of AD-MSCs, T-MSCs, 4T1 and VEGF (10 ng/ml) (A). The percent of wound closure was calculated after 4, 24, 48 and 72 hours relative

hour 0. VEGF induced the fastest healing rate with 100% closure after 48 hours (*: p value=0.02). T-MSCs and 4T1 with similar rates induced 88.02 and 78.23% closure after 72 hours. AD-MSCs induced 36.8% closure after 72 hours which was significantly lower compared to T-MSCs, 4T1 and VEGF (*: p value = 0.015) (B).

DISCUSSION

Tumoral Mesenchymal cells represent the supporting stroma of cancer (24-25). The role they play in tumor growth and invasion has recently become the center of interest regarding cancer biology and therapy (26). They are known to be responsible for immune evading properties of cancer by inducing regulatory T cells (27-28). It is shown that MSCs are recruited from surrounding tissues and the bone marrow in response to PDGF, IGF, RANTES and SDF-1 where they contribute to cancer growth (29-30).

As reports have previously shown, there are similarities between tumoral MSCs and adipose-derived MSCs (31); however, there are functional differences with respect to their surface markers, cytokine and enzyme productions.

Similar expressions of surface markers such asCD90, CD29, CD105, CD140a and Sca-1 indicate similar mesenchymal origin. Although MSCs were initially found to be negative for CD45 expression (32), Yu *et al.* showed that adult adipose derived MSCs express CD45 (33). Also, another study has shown that MSCs express CD45 when isolated and lose the expression of CD45 in consecutive *in vitro* cultures(34). Elevated levels of HLA-DR on the surface of tumor derived MSCs indicate that these cells may have the capability of interacting with immune cells directly. It also indicates that the tumor microenvironment is able to induce the expression of MHC-II. It has been shown that EGF-treated bone marrow-MSCs express MHC-II (35). Consistent with expression of EGF in cancers (36-37), it can be speculated that the expression of MHC-II in T-MSCs is the result of interaction with cancer microenvironment. It is very interesting that in the presence of TGF-β, IL10 and PGE2, all of which suppress MHC-II expression (31,38-40), this molecule is still expressed. This indicates thatadditional mechanisms and mediators may be involved in controlling MHC-II expression in the tumor microenvironment. Further studies are required to elucidate the underlying mechanism of MHC-II expression.

There have been many secreted mediators attributed to immune-suppression of MSCs. TGF-β, IL10, PGE2, Nitric Oxide in murine models and IDO in human MSCs are the main suppressors produced from MSCs (41). Our study, in accordance to previous studies, has shown the production of these mediators although not statistically significant (31,42). However, significant elevated level of PGE2 was observed in T-MSCs, which accompanied with TGF-β, could have additional effects. It has been shown that high PGE2 levels in cancer patients indicate higher invasiveness (43-44). With addition of TGF-β to the milieu, it can lead to Treg induction and increased IL10 production (45-46). Additionally, PGE2 is responsible for iNOS(47), MMP9 (48) and VEGF expression (49), which is evidenced by our results of Real-Time analysis and wound healing assay. Studies on colorectal cancers, as a model of COX-2-involved tumors, have shown the multifold actions of PGE2 in tumor initiation and development. COX-2/PGE2 pathway contributes to cancer cell survival, angiogenesis, invasion, metastasis and immune evasion (43). Studies have shown that inhibition of COX-2 in cancer models leads to increased efficacy of dendritic cell based vaccine treatment (50-51), increased CTL activity (52), and production ofIL12 and IFN-γ(53-54). There are several reasons for elevated levels of PGE2 in cancer: deregulated growth factor

signaling and oncogene activation, WNT pathway (55) and the Ras-MAPK pathway signaling (55-56) via growth factor receptors including EGFR (57), TGF-β (58), c-Met (59) and gastrin receptors (60). Also, the hypoxic microenvironment of cancer enhances the transcription of COX-2 via HIF-1 (61). Additionally, a recent study by Wong *et al*. demonstrated that within human tumor environment, Th1 type cells induce COX-2 expression in tumor derived myeloid-derived suppressor cells (MDSCs) as a counter-feedback mechanism via IFN-γ and TNF-α (62). They have demonstrated "an intrinsic mechanism underlying the self-limiting character of type-1 immunity within the human tumor environment". This self-limiting mechanism may be responsible for the limited success in cancer immunotherapies. This study showed that T-MSCs are also able to express COX-2 and produce PGE2. Whether this is linked to interactions with immune cells needs further study. This feedback mechanism is part of a normal process of immune system to limit the amount of tissue damage. However, in cancer, this mechanism is being used by the microenvironment to evolve and develop.

In conclusion, due to discrepancies in the results of cancer therapies using MSCs, gene and drug delivery in this system is still under investigation(19). Taking into account that there are unknown influences in various microenvironments, this discrepancy may be attributed to the microenvironment in which MSCs are intended for. Many studies take advantage of the fact that *in vivo* MSCs are able to migrate into inflamed tissue where the experimental inoculation of these cells indicate that the majority of i.v. inoculated MSCs accumulate in the lung (63). On the other hand, effective results were seen when local or simultaneous inoculations were used (64-66). Therefore, further studies on the properties of various niche and different models of cancer are needed to elucidate the mechanisms by which Mesenchymal cells contribute to the overall outcome of cancer therapy.

ACKNOWLEDGEMENTS

The funding for this study was provided by Tarbiat Modares University (Grant number: D52-1272-8.2.2010) and the support of Stem Cell Technology Research Center.

REFERENCES

1. Caplan AI. Adult mesenchymal stem cells for tissue engineering versus regenerative medicine. J Cell Physiol. 2007; 213:341-7.
2. Chamberlain G, Fox J, Ashton B, Middleton J. Concise review: mesenchymal stem cells: their phenotype, differentiation capacity, immunological features, and potential for homing. Stem Cells. 2007; 25:2739-49.
3. Rasmusson I, Ringdén O, Sundberg B, Le Blanc K. Mesenchymal stem cells inhibit the formation of cytotoxic T lymphocytes, but not activated cytotoxic T lymphocytes or natural killer cells. Transplantation. 2003; 76:1208-13.
4. Chiesa S, Morbelli S, Morando S, Massollo M, Marini C, Bertoni A, et al. Mesenchymal stem cells impair in vivo T-cell priming by dendritic cells. Proc Natl Acad Sci USA. 2011; 108:17384-9.
5. Krampera M, Glennie S, Dyson J, Scott D, Laylor R, Simpson E, et al. Bone marrow mesenchymal stem cells inhibit the response of naive and memory antigen-specific T cells to their cognate peptide. Blood. 2003; 101:3722-9.
6. Takahashi T, Tibell A, Ljung K, Saito Y, Gronlund A, Osterholm C, et al. Multipotent Mesenchymal Stromal Cells Synergize With Costimulation Blockade in the Inhibition of Immune

Responses and the Induction of Foxp3+ Regulatory T Cells. STEM CELL TRANSL MED. 2014; 3:1484-94.
7. Razmkhah M, Jaberipour M, Erfani N, Habibagahi M, Talei A-r, Ghaderi A. Adipose derived stem cells (ASCs) isolated from breast cancer tissue express IL-4, IL-10 and TGF-β1 and upregulate expression of regulatory molecules on T cells: do they protect breast cancer cells from the immune response? Cell Immunol. 2011; 266:116-22.
8. Spaggiari GM, Capobianco A, Abdelrazik H, Becchetti F, Mingari MC, Moretta L. Mesenchymal stem cells inhibit natural killer–cell proliferation, cytotoxicity, and cytokine production: role of indoleamine 2, 3-dioxygenase and prostaglandin E2. Blood. 2008; 111:1327-33.
9. Phinney DG. Functional heterogeneity of mesenchymal stem cells: implications for cell therapy. J Cell Biochem. 2012; 113:2806-12.
10. Elinav E, Nowarski R, Thaiss CA, Hu B, Jin C, Flavell RA. Inflammation-induced cancer: crosstalk between tumours, immune cells and microorganisms. Nature reviews Cancer. 2013; 13:759-71.
11. Kerkar SP, Restifo NP. Cellular constituents of immune escape within the tumor microenvironment. Cancer Res. 2012; 72:3125-30.
12. Castro-Malaspina H, Ebell W, Wang S. Human bone marrow fibroblast colony-forming units (CFU-F). Prog Clin Biol Res. 1983;154:209-36.
13. Mishra PJ, Mishra PJ, Humeniuk R, Medina DJ, Alexe G, Mesirov JP, et al. Carcinoma-associated fibroblast–like differentiation of human mesenchymal stem cells. Cancer Res. 2008; 68:4331-9.
14. Son BR, Marquez-Curtis LA, Kucia M, Wysoczynski M, Turner AR, Ratajczak J, et al. Migration of bone marrow and cord blood mesenchymal stem cells in vitro is regulated by stromal-derived factor-1-CXCR4 and hepatocyte growth factor-c-met axes and involves matrix metalloproteinases. Stem Cells. 2006; 24:1254-64.
15. Dwyer R, Potter-Beirne S, Harrington K, Lowery A, Hennessy E, Murphy J, et al. Monocyte chemotactic protein-1 secreted by primary breast tumors stimulates migration of mesenchymal stem cells. Clin Cancer Res. 2007; 13:5020-7.
16. Paunescu V, Bojin FM, Tatu CA, Gavriliuc OI, Rosca A, Gruia AT, et al. Tumour-associated fibroblasts and mesenchymal stem cells: more similarities than differences. J Cell Mol Med. 2011; 15:635-46.
17. Yu G, Wu X, Dietrich MA, Polk P, Scott LK, Ptitsyn AA, et al. Yield and characterization of subcutaneous human adipose-derived stem cells by flow cytometric and adipogenic mRNA analyzes. Cytotherapy. 2010; 12:538-46.
18. Yeh S, Chang J, Lo W, Liaw Y, Lin C, Lee C, et al. Induction of CD45 expression on bone marrow-derived mesenchymal stem cells. Leukemia. 2006; 20:894-6.
19. Dighe P, Viswanathan P, Mruthunjaya A, Seetharam R. Effect of bFGF on HLA-DR expression of human bone marrow-derived mesenchymal stem cells. Journal of stem cells. 2012; 8:43-57.
20. Goswami S, Sahai E, Wyckoff JB, Cammer M, Cox D, Pixley FJ, et al. Macrophages promote the invasion of breast carcinoma cells via a colony-stimulating factor-1/epidermal growth factor paracrine loop. Cancer Res. 2005; 65:5278-83.
21. Mao Y, Sarhan D, Steven A, Seliger B, Kiessling R, Lundqvist A. Inhibition of tumor-derived prostaglandin-E2 blocks the induction of myeloid-derived suppressor cells and recovers natural killer cell activity. Clin Cancer Res. 2014; 20:4096-106.
22. Hashemi SM, Hassan ZM, Pourfathollah AA, Soudi S, Shafiee A, Soleimani M. Comparative immunomodulatory properties of adipose-derived mesenchymal stem cells conditioned media from BALB/c, C57BL/6, and DBA mouse strains. J Cell Biochem. 2013; 114:955-65.
23. Greenhough A, Smartt HJ, Moore AE, Roberts HR, Williams AC, Paraskeva C, et al. The COX-2/PGE2 pathway: key roles in the hallmarks of cancer and adaptation to the tumour microenvironment. Carcinogenesis. 2009; 30:377-86.
24. Fang L, Chang H-M, Cheng J-C, Leung PC, Sun Y-P. TGF-β1 induces COX-2 expression and PGE2 production in human granulosa cells through Smad signaling pathways. J Clin Endocrinol Metab. 2014; 99:E1217-26.
25. Timoshenko AV, Lala PK, Chakraborty C. PGE2-mediated upregulation of iNOS in murine breast cancer cells through the activation of EP4 receptors. Int J Cancer. 2004;108:384-9.
26. Dempke W, Rie C, Grothey A, Schmoll H-J. Cyclooxygenase-2: a novel target for cancer chemotherapy? J Cancer Res Clin Oncol. 2001;127:411-7.
27. Toomey D, Murphy J, Conlon K. COX-2, VEGF and tumour angiogenesis. The Surgeon. 2009;7:174-80.

28. Basu GD, Tinder TL, Bradley JM, Tu T, Hattrup CL, Pockaj BA, et al. Cyclooxygenase-2 inhibitor enhances the efficacy of a breast cancer vaccine: role of IDO. J Immunol. 2006;177:2391-402.
29. Eberstål S, Fritzell S, Sandén E, Visse E, Darabi A, Siesjö P. Immunizations with unmodified tumor cells and simultaneous COX-2 inhibition eradicate malignant rat brain tumors and induce a long-lasting CD8(+) T cell memory. J Neuroimmunol. 2014;274:161-7.
30. Masferrer JL, Leahy KM, Koki AT, Zweifel BS, Settle SL, Woerner BM, et al. Antiangiogenic and antitumor activities of cyclooxygenase-2 inhibitors. Cancer Res. 2000;60:1306-11.
31. Wong J, Obermajer N, Edwards R, Bartlett D, Kalinski P. Activation of the COX2/PGE2 axis by immune effector cells promotes the self-limiting nature of type-1 immunity in cancer tissues The Journal of Immunology. 2014;192:73:1.
32. Eggenhofer E, Luk F, Dahlke MH, Hoogduijn MJ. The Life and Fate of Mesenchymal Stem Cells. FIMMU. 2014; 19:5:148.
33. Ren C, Kumar S, Chanda D, Kallman L, Chen J, Mountz JD, et al. Cancer gene therapy using mesenchymal stem cells expressing interferon-β in a mouse prostate cancer lung metastasis model. Gene Ther. 2008; 15:1446-53.
34. Nakamizo A, Marini F, Amano T, Khan A, Studeny M, Gumin J, et al. Human bone marrow–derived mesenchymal stem cells in the treatment of gliomas. Cancer Res. 2005;65:3307-18.
35. Studeny M, Marini FC, Champlin RE, Zompetta C, Fidler IJ, Andreeff M. Bone marrow-derived mesenchymal stem cells as vehicles for interferon-β delivery into tumors. Cancer Res. 2002;62:3603-8.